Modeling of magnetic and chemical ordering in binary alloys

J. M. Sanchez and C. H. Lin
Henry Krumb School of Mines, Columbia University, New York, New York 10027
(Received 14 February 1984)

The equilibrium properties of a model fcc binary alloy with two magnetic components are investigated using the tetrahedron approximation of the cluster-variation method. Temperature-composition phase diagrams are calculated for ordering alloys with both ferromagnetic and antiferromagnetic nearest-neighbor interactions. The interplay between magnetic and chemical long-range order is pronounced, affecting both the equilibrium phase diagram and the magnetic structure of the ordered states. The effect of chemical short-range order on the magnetic transitions is also analyzed.

I. INTRODUCTION

The interplay of magnetic and chemical ordering in alloys has been recognized for several years as an important element in the control of bulk magnetic properties. The available experimental evidence suggests that the effect of magnetic interactions in alloys is not negligible and will in general affect the equilibrium properties of the system.[1,2] Similar conclusions may be drawn from the results of recent theoretical studies[3–9] which incorporate the effect of coupling between magnetic and spatial ordering within the mean-field or Bragg-Williams approximation. These previous theoretical studies have demonstrated, for example, that magnetic interactions can cause chemical ordering even in the absence of chemical interactions.

Theoretical models of magnetic and spatial ordering based on the mean-field approximation are not, however, generally applicable to fcc systems for which short-range order plays a significant role. In fact, although the Bragg-Williams approximation provides a relatively accurate description of ferromagnetic systems and segregating alloys, it fails to reproduce the correct topology of the phase diagram for fcc antiferromagnets and ordering alloys. In addition, the mean-field approximation wrongly predicts the antiferromagnetic and/or ordering transitions at zero field to be second order.

The main objective of this work is to study the equilibrium properties of a model fcc alloy with two magnetic components and nearest-neighbor pair interactions using the tetrahedron approximation of the cluster-variation method (CVM).[10] In contrast to previous Bragg-Williams treatments, the tetrahedron approximation accurately describes the thermodynamic behavior of fcc systems with nearest-neighbor interactions for both ferromagnetic (segregating) and antiferromagnetic (ordering) systems. In this paper the emphasis is placed on the determination of the temperature-composition phase diagrams and on the analysis of short-range-order effects on the magnetic and ordering transition temperatures. Although the Hamiltonian used in our calculations is undoubtedly an oversimplification of the interactions present in real alloys, the general features observed in the experimental Ni-Fe phase diagram are closely reproduced by the model.

II. ENERGY MODEL AND GROUND STATES

We consider a binary fcc alloy with magnetic components A and B. The atomic species and the magnetic moment at a given lattice point p will be characterized, respectively, by a chemical occupation operator $\sigma(p)$ and by a spin operator $S(p)$. The occupation operator $\sigma(p)$ equals 1 for A atoms and -1 for B atoms. Furthermore, we will restrict our discussion to the case in which the spin for both components is $\frac{1}{2}$ and define $S(p)=\pm 1$.

For simplicity, we assume that the chemical and magnetic properties of the system are described by uncoupled Ising-model Hamiltonians with only nearest-neighbor pair interactions. Thus, the total configurational energy is given by

$$H=H_{\text{mag}}+H_{\text{chem}} . \tag{1}$$

In the absence of external magnetic fields, the magnetic-energy contribution is of the form

$$H_{\text{mag}}=\tfrac{1}{2}\sum_{p,p'} J(p-p')S(p)S(p') , \tag{2}$$

where the exchange integral between lattice sites p and p' is given by

$$J(p-p')=\sum_{i,j} J(i,j)\gamma(i,p)\gamma(j,p') \tag{3}$$

with $J(i,j)$ the nearest-neighbor exchange integral between species i and j, and where the occupation number $\gamma(i,p)$ equals 1 if lattice point p is occupied by an i atom and 0 otherwise. Using the convention that i is equal to 1 for A and -1 for B atoms, we may write $\gamma(i,p)$ as

$$\gamma(i,p)=\tfrac{1}{2}[1+i\sigma(p)] . \tag{4}$$

The chemical contribution to the energy is given by

$$H_{\text{chem}}=\tfrac{1}{2}V\sum_{p,p'} \sigma(p)\sigma(p') , \tag{5}$$

where the sum is over all nearest-neighbor pairs p and p', and where the effective pair interaction V is given by

$$V=\tfrac{1}{4}(V_{AA}+V_{BB}-2V_{AB}) \tag{6}$$

with V_{ij} denoting the interaction energy for an i-j pair.

The two limiting cases for which either the magnetic or the chemical interactions are identically zero have been extensively investigated by high-temperature expansion techniques,[11] cluster-variation-method calculations,[10,12–14] and Monte Carlo simulations.[15,16] For negative nearest-neighbor interactions, the stable state at $T=0$ K (ground state) is ferromagnetic for the magnetic system ($J<0$, $V=0$) and completely segregated for the binary alloy case ($V<0$, $J=0$). On the other hand, for positive nearest-neighbor interactions the magnetic ground state at zero field is a type-I antiferromagnet and the ground states of the binary alloy are the $L1_0$ and $L1_2$ ordered structures occurring, respectively, at stoichiometries AB and A_3B (or AB_3).

The determination of the ground states of the total Hamiltonian can be formulated as a relatively straightforward problem in linear programming.[17–20] Such ground states are well known for the binary fcc lattice with up to fourth neighbor pair and/or many-body interactions. If only nearest-neighbor interactions are included, the lowest-energy states may occur for the pure elements and for ordered structures of stoichiometries A_3B, AB, and AB_3. In this approximation the ordered ground states are degenerate, with the highest symmetry structures corresponding to the $L1_0$ (CuAu) and $L1_2$ (Cu_3Au) structures.

When both chemical and magnetic interactions are present, each of the stoichiometric binary ground states may adopt a ferromagnetic or antiferromagnetic structure (of either type I or type II) depending on the values of the exchange integrals $J(i,j)$. A list of all possible ground states at stoichiometries A, A_3B, AB, AB_3, and B is given in Table I. In the first column of Table I, the ground-state structures are characterized by the chemical species and magnetic moment at each of the four equivalent lattice sites in the fcc unit cell. In the second column of Table I the energy of the ground-state structures relative to that of an ideal mixture (i.e., the energy of formation) is given. The third column gives the range of magnetic interactions for which the structure in question may be expected to be stable at $T=0$ K. The stability of the structure will also depend on the value of the chemical interaction V, the criterion for stability being that the energy of formation (second column of Table I) be lower than the energy of a mixture with the same overall concentration of any pair of ground states.

The finite-temperature behavior of the model is investigated within the tetrahedron approximation of the cluster-variation method. The CVM was first proposed by Kikuchi in 1951 (Ref. 10) and, since then, has been applied to several binary and ternary alloy systems.[12–14,21–24] In particular, the tetrahedron approximation applied to the fcc lattice with nearest-neighbor interaction gives results in good agreement with Monte Carlo simulations.[14] For example, the ordering temperatures at the stoichiometric compositions obtained by the two methods differ by approximately 5%, with the major discrepancies taking place near an apparently singular ($T=0$ K) triple point.

For all cases investigated in this article, the states of magnetic and spatial long-range order can be described by introducing two sublattices, α and β, which reflect the symmetry of the $L1_0$ or the $L1_2$ ordered structures. The chemical (η_c) and antiferromagnetic (η_m) long-range order parameters may be defined in terms of the sublattice averages of the occupation and spin operators as

$$\eta_m=\tfrac{1}{2}[\langle S(p_\alpha)\rangle-\langle S(p_\beta)\rangle] \tag{7}$$

and

TABLE I. Possible ground states of a binary fcc magnetic alloy with nearest-neighbor interactions.

Structure	$\Delta H=H-(c_AH_A+c_BH_B)$	Stability range
$A\uparrow A\uparrow A\uparrow A\uparrow$		$J_{AB}<0$
$A\uparrow A\uparrow A\downarrow A\downarrow$		$J_{AB}>0$
$A\uparrow A\uparrow A\uparrow B\uparrow$	$-6V-(3J_{AA}+3J_{BB}-6J_{AB})/2$	$J_{AA}<0,J_{BB}<0,J_{AB}<0$
	$-6V+(9J_{AA}+J_{BB}+6J_{AB})/2$	$J_{AA}>0,J_{BB}>0,J_{AB}<-2J_{AA}$
	$-6V+(9J_{AA}-3J_{BB}+6J_{AB})/2$	$J_{AA}>0,J_{BB}<0,J_{AB}<-2J_{AA}$
$A\uparrow A\uparrow A\uparrow B\downarrow$	$-6V-(3J_{AA}+3J_{BB}+6J_{AB})/2$	$J_{AA}<0,J_{BB}<0,J_{AB}>0$
	$-6V+(9J_{AA}+J_{BB}-6J_{AB})/2$	$J_{AA}>0,J_{BB}>0,J_{AB}>2J_{AA}$
	$-6V+(9J_{AA}-3J_{BB}-6J_{AB})/2$	$J_{AA}>0,J_{BB}<0,J_{AB}>2J_{AA}$
$A\uparrow A\uparrow A\downarrow B\uparrow$	$-6V+(3J_{AA}+3J_{BB}+6J_{AB})/2$	$J_{AA}>0,J_{BB}>0,-2J_{AA}<J_{AB}<0$
	$-6V+(J_{AA}-3J_{BB}+2J_{AB})/2$	$J_{AA}>0,J_{BB}<0,-2J_{AA}<J_{AB}<0$
$A\uparrow A\uparrow A\downarrow B\downarrow$	$-6V+(J_{AA}+J_{BB}-2J_{AB})/2$	$J_{AA}>0,J_{BB}>0,0<J_{AB}<2J_{AA}$
	$-6V+(J_{AA}-3J_{BB}-2J_{AB})/2$	$J_{AA}>0,J_{BB}<0,0<J_{AB}<2J_{AA}$
$A\uparrow A\uparrow B\uparrow B\uparrow$	$-8V-(2J_{AA}+2J_{BB}-4J_{AB})$	$J_{AA}<0,J_{BB}<0,J_{AB}<0$
	$-8V+(2J_{AA}+2J_{BB}+4J_{AB})$	$J_{AA}>0,J_{BB}>0,J_{AB}<-(J_{AA}+J_{BB})/2$
	$-8V+(2J_{AA}-2J_{BB}+4J_{AB})$	$J_{AA}>0,J_{BB}<0,J_{AB}<-J_{AA}/2$
$A\uparrow A\uparrow B\downarrow B\downarrow$	$-8V-(2J_{AA}+2J_{BB}+4J_{AB})$	$J_{AA}<0,J_{BB}<0,J_{AB}>0$
	$-8V+(2J_{AA}+2J_{BB}-4J_{AB})$	$J_{AA}>0,J_{BB}>0,J_{AB}>(J_{AA}+J_{BB})/2$
	$-8V+(2J_{AA}-2J_{BB}-4J_{AB})$	$J_{AA}>0,J_{BB}<0,J_{AB}>J_{AA}/2$
$A\uparrow A\downarrow B\uparrow B\downarrow$	$-8V$	$J_{AA}>0,J_{BB}>0,-1<2J_{AB}/(J_{AA}+J_{BB})<1$
$A\downarrow A\uparrow B\uparrow B\uparrow$	$-8V-2J_{BB}$	$J_{AA}>0,J_{BB}<0,-1<2J_{AB}/J_{AA}<1$

$$\eta_c = \tfrac{1}{2}[\langle\sigma(p_\alpha)\rangle - \langle\sigma(p_\beta)\rangle] \,. \tag{8}$$

Finally, calling θ the fraction of α sites we may write the total magnetization per lattice point (m) and the average concentration of species i (c_i) as

$$m = \theta\langle S(p_\alpha)\rangle + (1-\theta)\langle S(p_\beta)\rangle \,, \tag{9}$$

$$c_i = \theta\langle\gamma(i,p_\alpha)\rangle + (1-\theta)\langle\gamma(i,p_\beta)\rangle \,. \tag{10}$$

III. RESULTS

In reference to the ground states listed in Table I, phase diagrams were calculated for ordering magnetic alloys ($V>0$) with ferromagnetic interactions (J_{AA}, J_{AB}, and $J_{BB}<0$) and with mixed magnetic interactions ($J_{AB}, J_{BB}<0$, and $J_{AA}>0$). The calculated temperature-chemical potential and temperature-concentration phase diagrams are shown in Figs. 1–3. A summary of the interaction energy parameters used in each case is given in Table II. In addition, the temperature dependence of the chemical and magnetic long-range order parameters and the total magnetization defined, respectively, by Eqs. (7), (8), and (9), are shown for various values of chemical potentials (concentrations) in Fig. 4.

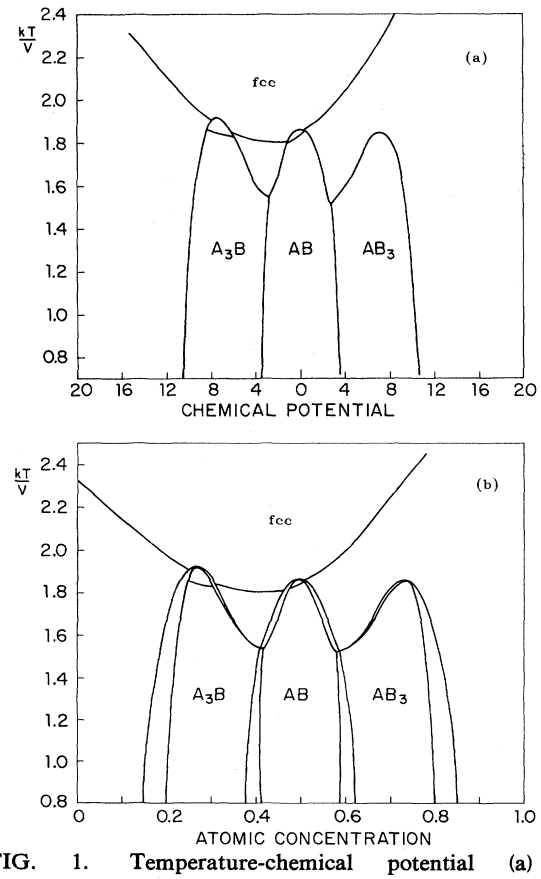

FIG. 1. Temperature-chemical potential (a) and temperature-concentration (b) phase diagrams for $V>0$, $J_{AA}=-0.232V$, $J_{AB}=-0.126V$, and $J_{BB}=-0.306V$. The transition line at high temperatures (second order) corresponds to the Curie temperature. At low temperatures all phases are ferromagnetic.

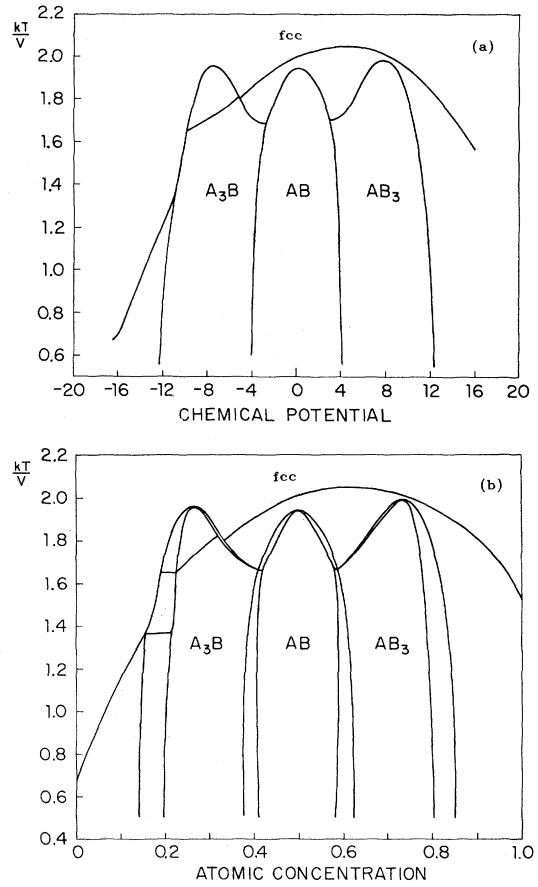

FIG. 2. Temperature-chemical potential (a) and temperature-concentration (b) phase diagrams for $V>0$, $J_{AA}=-0.066V$, $J_{AB}=-0.260V$, and $J_{BB}=-0.153V$. The transition line at high temperatures (second order) corresponds to the Curie temperature. At low temperatures all phases are ferromagnetic.

The overall behavior of the Curie temperature with concentration seen in the phase diagrams of Figs. 1–3 can be understood in terms of a simplified model with concentration and short-range-order–dependent exchange interactions. We define an effective magnetic Hamiltonian by averaging the energy of the system with respect to the spatial configurational variables $\sigma(p)$. The effective magnetic energy is then given by

$$\langle H\rangle_{\text{mag}} = \tfrac{1}{2}\sum_{p,p'} \tilde{J}(p-p')S(p)S(p') \,, \tag{11}$$

where the average exchange integral $\tilde{J}(p-p')$ is given by

TABLE II. Nearest-neighbor magnetic interactions used for the calculation of the phase diagrams shown in Figs. 1 to 3. The effective chemical interaction V is taken to be positive.

Figure	J_{AA}/V	J_{AB}/V	J_{BB}/V	J_2/V
1	−0.232	−0.126	−0.306	−0.071
2	−0.066	−0.260	−0.153	0.075
3	0.225	−0.470	−0.230	0.234

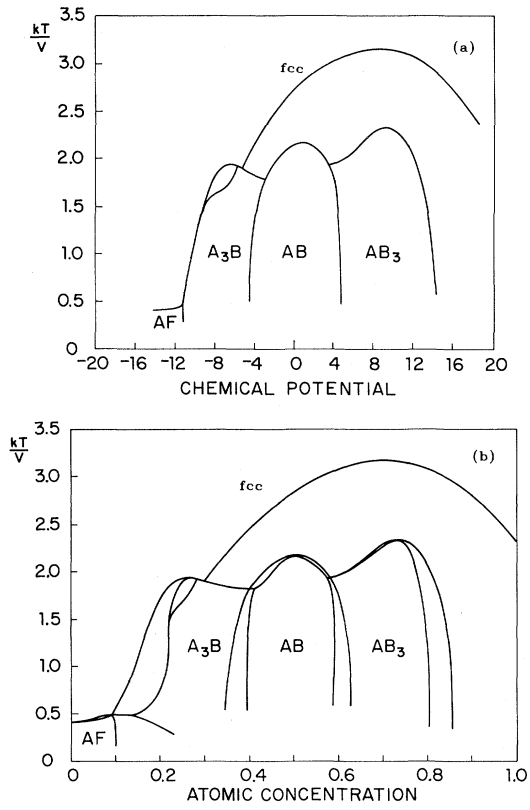

FIG. 3. Temperature-chemical potential (a) and temperature-concentration (b) phase diagrams for $V>0$, $J_{AA}=0.225V$, $J_{AB}=-0.470V$, and $J_{BB}=-0.230V$. The disordered phase is antiferromagnetic in the low-temperature and low-concentration range. For concentrations above approximately 0.1, all phases are ferromagnetic at $T=0$ K.

$$\tilde{J}(p-p')=\sum_{i,j}J(i,j)\langle\gamma(i,p)\gamma(j,p')\rangle$$
$$=\sum_{i,j}J(i,j)y(i,j) \tag{12}$$

with $y(i,j)$ the probability of finding an i-j nearest-neighbor pair.

Neglecting the temperature (or short-range order) dependence of the average exchange interaction $\tilde{J}$, the magnetic transition temperature for the Hamiltonian (11) is given by

$$k_B T_m=\tau\tilde{J}\ , \tag{13}$$

where in the tetrahedron approximation the proportionality constant τ is equal to 10.025 for ferromagnetic ($\tilde{J}<0$) and 1.892 for antiferromagnetic systems ($\tilde{J}>0$).

In general, the average exchange integral $\tilde{J}$ will depend on temperature and concentration in a complicated manner. However, a simple dependence of $\tilde{J}$ on average concentration, or $\langle\sigma(p)\rangle$, and on the short-range order parameter $\langle\sigma(p)\sigma(p')\rangle$ can be made explicit by incorporating the definition of $\gamma(i,p)$ into Eq. (12):

$$\tilde{J}=J_0+2J_1\langle\sigma(p)\rangle+J_2\langle\sigma(p)\sigma(p')\rangle\ , \tag{14}$$

where

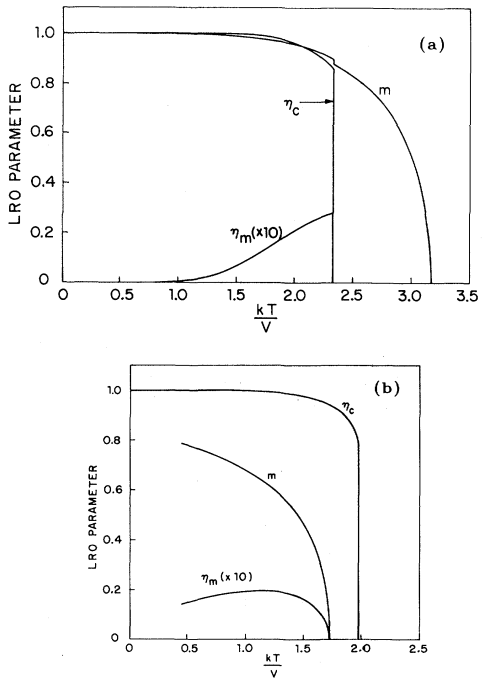

FIG. 4. Total magnetization (m), chemical long-range order (η_c), and antiferromagnetic long-range order (η_m) parameters as a function of temperature for the case depicted in Fig. 3 ($J_{AA}=0.225V$, $J_{AB}=-0.470V$, and $J_{BB}=-0.230V$) at chemical potentials equal to 8.4 (a) and -6 (b).

$$J_0=\tfrac{1}{4}(J_{AA}+J_{BB}+2J_{AB})\ ,$$
$$J_1=\tfrac{1}{4}(J_{AA}-J_{BB})\ ,$$
$$J_2=\tfrac{1}{4}(J_{AA}+J_{BB}-2J_{AB})\ .$$

If the paramagnetic-to-ferromagnetic transition occurs at high temperatures relative to the ordering transition, one expects the effect of short-range order on the Curie temperature to be small. Specifically, the nearest-neighbor correlation function $\langle\sigma(p)\sigma(p')\rangle$ will be approximately given by $\langle\sigma(p)\rangle^2$ and the loci of T_m versus concentration will be parabolic with a maximum or minimum occurring at $\langle\sigma(p)\rangle=-J_1/J_2$ or $c_B=(J_1+J_2)/(2J_2)$. This nearly parabolic behavior of the Curie temperature is apparent for the calculated phase diagrams shown in Figs. 1–3.

The effect of the ordering transition on the Curie temperature near critical end points can also be understood in terms of Eq. (13) and the changes induced by long-range order on the effective exchange integral. Assuming the same average concentration [or $\langle\sigma(p)\rangle$] for the ordered and disorderd phases, the change in $\tilde{J}$ due to the onset of long-range order is given by

$$\Delta\tilde{J}=J_2\Delta\langle\sigma(p)\sigma(p')\rangle\ , \tag{15}$$

where the discontinuous change in the pair correlation, $\Delta\langle\sigma(p)\sigma(p')\rangle$, is negative. Thus, for negative values of J_2 (and $\tilde{J}$) it follows that $|\tilde{J}(\text{ord})|<|\tilde{J}(\text{dis})|$ and the Curie temperature will decrease on ordering (see Fig. 1). The opposite behavior, i.e., an increase in T_m on ordering, is

seen in Figs. 2–3 for positive values of J_2. (Note that $\tilde{J}<0$ for all cases investigated, except at low concentrations in Fig. 3.)

Another important effect caused by the interplay of chemical and magnetic interactions is the induced asymmetry, absent in the nonmagnetic alloy, in the A_3B and AB_3 transition temperatures. Averaging the total Hamiltonian over the spin configurations we obtain the following effective Hamiltonian for the binary alloy:

$$\langle H\rangle_{\text{chem}}=\tilde{V}\sum_{p,p'}\sigma(p)\sigma(p')\ , \tag{16}$$

with the effective chemical interaction given by

$$\tilde{V}=V+J_2\langle S(p)S(p')\rangle\ . \tag{17}$$

The transition temperatures for the A_3B and AB_3 ordering reactions are approximately given by

$$k_BT_0=\tau\tilde{V}\ ,$$

where in the tetrahedron approximation and for positive $\tilde{V}$ the constant τ equals 1.892 for $L1_0$ and 1.925 for the $L1_2$ transitions.

For all three cases investigated, the disordered phases are paramagnetic at the A_3B transition and ferromagnetic at the AB_3 transition. Thus, neglecting spin correlations in the high-temperature paramagnetic phase and taking $\langle S(p)S(p')\rangle=1$ in the ferromagnetic state, we may approximate the ratio of transition temperatures by

$$T_0(AB_3)/T_0(A_3B)=(V+J_2)/V\ . \tag{18}$$

Figure 1 illustrates the case of negative J_2 which results in a higher ordering temperature for the A_3B structure relative to AB_3. Two cases for which $T_0(AB_3)>T_0(A_3B)$, i.e., for positive J_2, are shown in Fig. 2 ($J_2=0.075V$) and Fig. 3 ($J_2=0.234V$). Note that the asymmetry is more pronounced in the phase diagram of Fig. 3 for which the AB_3 transition takes place deeper into the ferromagnetic phase.

As mentioned in the Introduction, magnetic interactions play a significant role on the equilibrium properties of alloys since they may induce spatial ordering even in the absence of chemical interactions. Conversely, chemical long-range order may also significantly affect the magnetic structure of the alloy as seen in the long-range order parameters versus composition plots shown in Fig. 4. Specifically, the antiferromagnetic long-range order parameter η_m is different from 0 for the magnetic ordered alloy at finite temperatures, although the ordered ground state is ferromagnetic. The onset of antiferromagnetic long-range order is discontinuous if the high-temperature chemically disordered phase is ferromagnetic [Fig. 4(a)] and continuous if the magnetic transition takes place in the chemically ordered phase [Fig. 4(b)]. The antiferromagnetic long-range order parameter is seen to decrease at low temperatures and according to the ground-state analysis (Table I) it vanishes at $T=0$ K.

IV. SUMMARY

A simple nearest-neighbor pairwise model for a binary magnetic alloy with fcc structure was investigated using the tetrahedron approximation of the cluster-variation method. Contrary to the Bragg-Williams approximation used previously for the simultaneous treatment of magnetic and chemical interactions in the fcc lattice, the tetrahedron approximation gives results that are qualitatively correct and which are expected to be accurate within 5% near stoichiometric points. As suggested by Monte Carlo simulations in nonmagnetic binary systems, the error in the calculated phase diagrams may be larger near the triple point where the disordered and the two ordered structures coexist.

As emphasized previously by several authors, the interplay between both types of interactions significantly affects the equilibrium properties of the system. In particular, magnetic interactions will generally induce an asymmetry in the equilibrium phase diagram that is absent in the pairwise model for nonmagnetic systems. Our calculations also indicate that chemical long-range order will result in the onset of antiferromagnetic long-range order even when the lowest-energy ordered state at $T=0$ K is ferromagnetic.

Although the Hamiltonian used in our model is not expected to be applicable to real alloys, the equilibrium phase diagram shown in Fig. 3 closely resembles the Ni-rich portion (fcc) of the experimental Ni-Fe phase diagram. A detailed investigation of this system is currently under way and the results will be reported in a forthcoming publication.

ACKNOWLEDGMENTS

This work was funded by the National Science Foundation (NSF) under Grant No. DMR-82-06195. The authors wish to thank Dr. Robert Reynik of NSF for his support.

[1]T. W. McDaniel and C. L. Foiles, Solid State Commun. **14**, 835 (1974).
[2]C. R. Houska, J. Phys. Chem. Solids **24**, 95 (1963).
[3]G. Inden, in *Alloy Phase Diagrams*, Materials Research Society Symposia Proceedings, edited by L. H. Bennett, T. B. Massalski, and B. C. Giessen (North-Holland, New York, 1983), Vol. 19, p. 175.
[4]J. Urias and J. L. Moran-Lopez, Phys. Rev. B **26**, 2669 (1982).
[5]L. Billard, P. Villemain, and A. Chamberod, J. Phys. C **11**, 2815 (1978).
[6]R. Tahir-Kheli and T. Kawasaki, J. Phys. C **10**, 2207 (1977).
[7]J. L. Moran-Lopez and L. M. Falicov, J. Phys. C **13**, 1715 (1980).
[8]J. L. Moran-Lopez and L. M. Falicov, Solid State Commun. **31**, 325 (1979).
[9]F. Mejia-Lira, J. Urias, and J. L. Moran-Lopez, Phys. Rev. B **24**, 5270 (1981).
[10]R. Kikuchi, Phys. Rev. B **81**, 988 (1951).
[11]C. Domb and M. S. Green, *Phase Transition and Critical Phenomena* (Academic, London, 1971).

[12]J. M. Sanchez and D. de Fontaine, Phys. Rev. B **25**, 1759 (1982).
[13]C. M. van Baal, Physica (Utrecht) **64**, 571 (1973).
[14]J. M. Sanchez, W. Teitler, and D. de Fontaine, Phys. Rev. B **26**, 1465 (1982).
[15]K. Binder, Phys. Rev. Lett. **45**, 811 (1980).
[16]K. Binder, J. L. Lebowitz, M. K. Phani, and M. H. Kalos, Acta Metall. **29**, 1655 (1981).
[17]M. J. Richard and J. W. Cahn, Acta Metall. **19**, 1263 (1971).
[18]S. M. Allen and J. W. Cahn, Acta Metall. **20**, 423 (1972).
[19]J. Kanamori, Prog. Theor. Phys. **35**, 66 (1966).
[20]J. M. Sanchez and D. de Fontaine, in *Structure and Bonding in Crystals,* edited by M. O'Keefe and A. Navrotsky (Academic, New York, 1981), Vol. II, p. 117.
[21]J. M. Sanchez and D. de Fontaine, Phys. Rev. B **21**, 216 (1980).
[22]J. M. Sanchez and D. de Fontaine, Phys. Rev. B **25**, 1759 (1982).
[23]R. Kikuchi, J. M. Sanchez, D. de Fontaine, and H. Yamauchi, Acta Metall. **28**, 651 (1980).
[24]C. Sigli and J. M. Sanchez, Computer Coupling of Phase Diagrams and Thermochemistry (CALPHAD) (to be published).